On the origin of surface ozone and reactive nitrogen observed at a remote mountain site in the northeastern Qinghai-Tibetan Plateau, western China

T. Wang,[1] H. L. A. Wong,[1] J. Tang,[2] A. Ding,[1] W. S. Wu,[1] and X. C. Zhang[2]

Received 25 July 2005; revised 25 November 2005; accepted 11 January 2006; published 28 April 2006.

[1] Measurements of surface ozone (O_3), carbon monoxide (CO), nitric oxide (NO), and total reactive nitrogen (NO_y) were made, in conjunction with other trace gases and fine aerosols, at Mount Waliguan (WLG, 36.28°N, 100.90°E, 3816 m above sea level) in the late spring and summer of 2003 in order to better understand the source(s) of ozone and other chemically active gases over the remote highlands of western China. The average mixing ratio (plus or minus standard deviation) was 58 (±9) ppbv for O_3, 155 (±41) ppbv for CO, and 3.83 (±1.46) ppbv for NO_y in the spring phase, compared to a summer average value of 54 (±11) ppbv for O_3, 125 (±36) ppbv for CO, and 3.60 (±1.13) ppbv for NO_y. The daytime (0800–1759 local time) average NO mixing ratios were 72 (±79) pptv and 47 (±32) pptv in the spring and summer, respectively. The ozone mixing ratios exhibited a minimum in late morning, while CO (and NO_y in spring) showed enhanced concentrations at night. The latter is in contrast to the diurnal behaviors observed in many remote mountain sites. Analysis of 10-day back trajectories using output from Fifth-Generation National Center for Atmospheric Research/Penn State University Mesoscale Model (MM5) simulations shows that air masses from the remote western regions contained the lowest level of CO (121–129 ppbv) but had the highest O_3 (60 ppbv), compared to the other three air mass groups that were impacted by anthropogenic emissions in eastern/southern China and in the Indian subcontinent. Ozone correlated negatively with CO (and water vapor content), particularly during summer in air originating in the west, suggesting that the high-ozone events were mostly derived from the downward transport of the upper tropospheric air and not from anthropogenic pollution. An examination of in situ chemical measurements (CO-NO_y correlation, ethyne/propane, and benzene/propane) as well as Measurements of Pollution in the Troposphere (MOPITT) and Moderate-Resolution Imaging Spectroradiometer (MODIS) remote-sensing data revealed some impacts from forest fires in central Asia in the late spring of 2003 on the background concentrations of trace gases over western China. While the O_3 and CO levels at WLG are comparable to those at remote continental sites in Europe and North America, the NO_y concentrations were substantially higher at WLG. The possible reasons for the abnormally high NO_y levels are discussed. While more studies are needed to pin down these sources/causes, including a possible contribution from long-range transport, we believe that microbial processes in soils and animal wastes associated with animal grazing were an important cause of the elevated NO_y. The observed daytime NO concentrations imply a net photochemical production of O_3 at WLG, suggesting a positive contribution of photochemistry to the ozone budget.

Citation: Wang, T., H. L. A. Wong, J. Tang, A. Ding, W. S. Wu, and X. C. Zhang (2006), On the origin of surface ozone and reactive nitrogen observed at a remote mountain site in the northeastern Qinghai-Tibetan Plateau, western China, *J. Geophys. Res.*, *111*, D08303, doi:10.1029/2005JD006527.

1. Introduction

[2] Tropospheric ozone (O_3) is one of the most important trace gases with regard to regional air quality, atmospheric chemistry, and climate change. Elevated ground-level O_3 concentrations are known to have detrimental effects on human health, crops, and vegetation [*National Research Council*, 1991]. Ozone regulates the oxidative capacity of

[1]Department of Civil and Structural Engineering, Hong Kong Polytechnic University, Hong Kong, China.
[2]Key Laboratory for Atmospheric Chemistry, Centre for Atmosphere Watch and Services, Chinese Academy of Meteorological Sciences, Beijing, China.

0148-0227/06/2005JD006527

the atmosphere via the production of hydroxyl (OH) radicals, and it is also an effective greenhouse gas, particularly in the middle and upper troposphere, thus directly contributing to global warming [e.g., *Derwent et al.*, 2002].

[3] The budget of tropospheric O_3 is controlled by the downward transport of stratospheric air at an extratropical latitude [*Danielsen*, 1968], the depositional loss to the Earth's surface, and the oxidation of hydrocarbons and CO by OH radicals in the presence of oxides of nitrogen (NO_x, NO_x = NO + NO_2) [*Crutzen*, 1973]. The latter photochemical process can be either a source or sink for ozone, depending on the levels of NO_x. In the remote atmosphere where NO level is very low (e.g., <10 pptv), O_3 is destroyed by photolysis of O_3, followed by reactions among O_3, OH, HO_2, and RO_2

$$O_3 + h\nu(<320\ \text{nm}) \rightarrow O(^1D) + O_2$$

$$O(^1D) + H_2O \rightarrow OH + OH$$

$$OH + O_3 \rightarrow O_2 + HO_2$$

$$HO_2 + O_3 \rightarrow OH + 2O_2$$

In a NO_x-rich environment (e.g., NO > 50 ppbv), photochemistry leads to a net production of ozone via the reaction between NO with HO_2 and RO_2, followed by the photolysis of NO_2

$$HO_2 + NO \rightarrow NO_2 + OH$$

$$RO_2 + NO \rightarrow NO_2 + RO$$

$$NO_2 + h\nu(<420\ \text{nm}) \rightarrow O(3P) + NO$$

$$O(3P) + O_2 + M \rightarrow O_3 + M$$

Given the critical role of NO_x in determining the net effect of photochemistry on the ozone budget, a large number of studies have been conducted to measure the atmospheric concentrations of oxides of nitrogen, along with CO and hydrocarbons, and to quantify the role of photochemistry in different regions of the globe.

[4] With an average altitude of over 4000 m, the Qinghai-Tibetan Plateau is the highest landmass on Earth, and plays a key role in atmospheric circulation. The atmosphere lying over the Plateau is probably the least affected by human activities in the Asian continent because of the sparse population and minimal industrial activities in western China. Previous measurements of surface ozone have shown that concentrations peak in summer (June) at Mount Waliguan (WLG) in the northeastern edge of the plateau [*Tang et al.*, 1995]. This contrasts with the common spring maximum observed in most remote areas of the Northern Hemisphere [*Monks*, 2000]. While evidence such as rich ozone and low water vapor during the observed high-ozone events suggests an upper tropospheric/lower stratospheric source, and a modeling study using filter-based measurements of NO_2 implies a net destruction due to photochemistry [*Ma et al.*, 2002] in summer, direct measurements of nitric oxide are necessary in order to accurately determine the role of photochemistry in the ozone budget in the remote atmosphere of western China. In addition, measurements of anthropogenic tracers are needed to examine the potential impacts of the transport of regional pollution from populated eastern China and from other parts of the world.

[5] During April-May and July-August 2003, intensive measurements of CO, NO, NO_y, C_1-C_8 hydrocarbons, C_1-C_2 halocarbons, and fine aerosols were added to the ongoing monitoring of ozone, greenhouse gases, and meteorological parameters at WLG to better characterize the chemical compositions of the air masses arriving at the site and to better understand the source(s) of surface ozone and other trace gases in the western highlands of China. In this paper, we present the results of continuously measured ozone, CO, NO, and NO_y. Because of its intermediate lifetime of 1–2 months, CO is a useful tracer of combustion processes such as the burning of fossil fuel and biomass/biofuel. Total reactive nitrogen (NO_y = NO + NO_2 + NO_3 + $2N_2O_5$ + HONO + HO_2NO_2 + PAN + HNO_3 + aerosol nitrate + organic nitrate) is a more conserved quantity than individual NO_y species such as NO_x, and thus is a better representation of the total abundance of reactive nitrogen during transport. Concurrent measurements of NO_y with CO, O_3, and other tracers also provide valuable information on the sources of these compounds.

2. Experiment and Methodologies

2.1. Site Description

[6] The field study was carried out at the WLG Observatory, which is one of the World Meteorological Organization's (WMO) Global Atmospheric Watch (GAW) Baseline Stations. The Observatory is situated on the northeastern edge of the Qinghai-Tibetan Plateau (36.28°N, 100.90°E, 3816 m above sea level (asl); see Figure 1), and is on an isolated mountain peak stretching from northwest to southeast. The surrounding areas are naturally preserved arid/semiarid lands and scattered grasslands.

[7] WLG is isolated from the industrial and populated regions of China, with a population density of less than 6 people per square km [*Zhou et al.*, 2003]. The capital city of Qinghai Province, Xi'ning (2296 m asl), is located 90 km to the east, separated by several high mountains of approximately 4000 m asl (see Figure 1). No significant sources of pollutants are present to the west, except a township of Qiapu Qia (population: 30,000) located 26 km to the west but at an elevation of 1000 m below the station. An examination of CO as a function of wind direction showed no detectable enhancement of CO for a wind direction of 260–290 degrees, indicating a negligible impact on the trace gases measured during the study periods. Closer to the station, an altar was situated 200 m southeast of the station building. The CO and wind data did not suggest that the altar had a notable impact on the levels of trace gas during this study.

2.2. Measurement Techniques

[8] Measuring instruments were housed in a temperature-controlled laboratory at the second floor of the station. Ambient air samples were drawn through a perfluoroalkoxy (PFA) sampling tube (outside diameter, 12.7 mm; inside diameter, 9.6 mm; length, 9.3 m). The inlet was installed at 3 m above the rooftop of the station. Inside the laboratory,

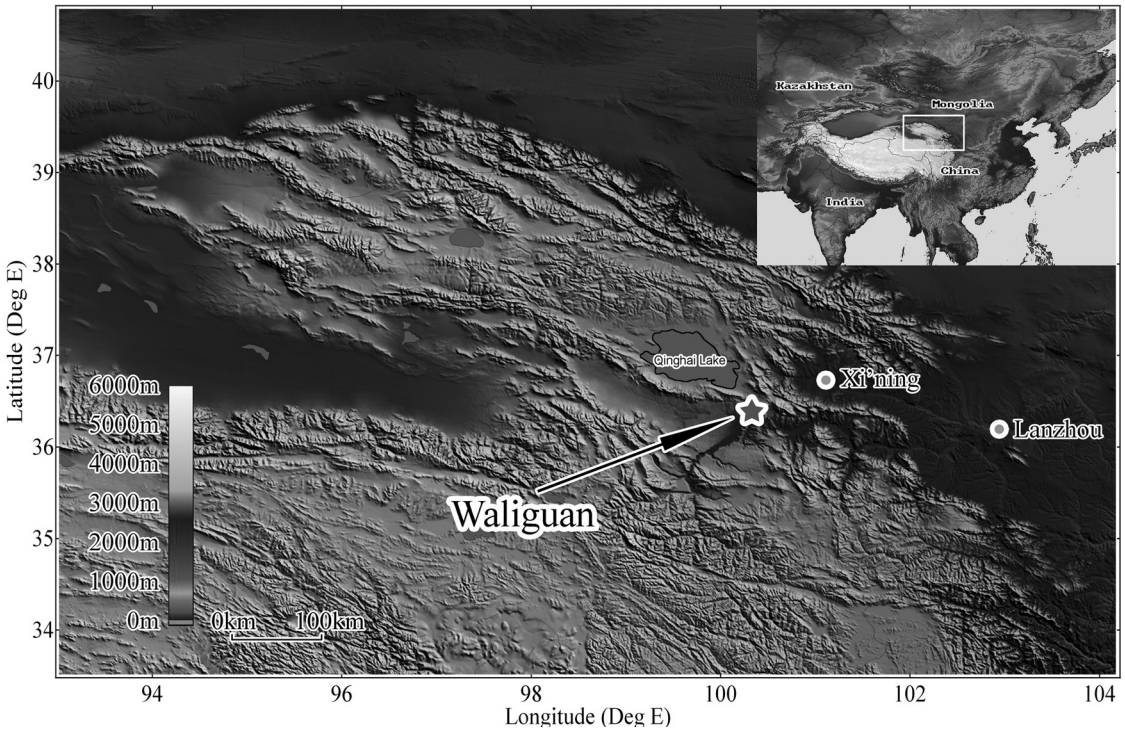

Figure 1. Map showing the study site and the surrounding regions.

the sampling tube was connected to a PFA-made manifold with a bypass pump drawing air at the rate of 7.9 L/min to reduce the residence time of sampled air. The intakes of the CO and NO analyzer were connected to the manifold, while a separate inlet box that housed the catalytic converter for NO_y and calibration valves was installed at 1.8 m above the rooftop, with a sample line length of 13.5 m (flow = 1.5 L/min, inside diameter: 3.2 mm). The sample inlet for the routinely measured O_3 was located at the same rooftop, next to the sample inlets for the NO, NO_y, and CO analyzers. Meteorological instruments were installed on a tower next to the station building: a wind sensor for measuring both horizontal and vertical winds was located at a height of 20 m, and temperature, pressure and relative humidity (RH) sensors were located at a height of 2.3 m.

[9] O_3 was measured using a commercial UV photometric analyzer (Thermal Environmental Instruments (TEI) Model 49), which had a detection limit of 2 ppbv with a precision of 2 ppbv. The analyzer was calibrated following the protocol developed for the WMO-GAW network.

[10] CO was measured with a gas filter correlation, nondispersive infrared analyzer (Advanced Pollution Instrumentation (API), Model 300) with a heated catalytic scrubber to convert CO to carbon dioxide (CO_2) for baseline determination. The detection limit was 30 ppbv for a 2-min average, with a 2-σ precision of about 1% for a level of 500 ppbv (2-min average) and an overall uncertainty of 10% [*Wang et al.*, 2001a]. The CO analyzer was calibrated on a daily basis by injecting scrubbed ambient air (produced from TEI, Model 111) and a span gas generated by diluting an US National Institute of Standards and Technology traceable standard (containing 147.4 ppmv CO (±2%), 15.05 ppmv NO (±2%), and 14.65 ppmv SO_2 (±2%), purchased from Scott-Marrin Inc., California). The baseline for CO was determined by passing ambient air to the internal scrubber every hour, each lasting 20 min. The CO concentrations were also separately determined during the analyses of 119 canister samples at D. Blake's laboratory at the University of California, Irvine, using the gas chromatographic methods. The continuous and canister CO values show a good agreement ($[CO]_{API} = 1.1\ [CO]_{canister} - 21$, r = 0.95) with an average API-to-canister ratio of 0.959.

[11] NO was detected with a chemiluminescence analyzer (Eco Physics, Model CLD 770 AL ppt), which had a limit of detection of 15 pptv (S/N = 2) for an integration time of 5 min, with a 2-σ precision of 10% and an uncertainty of 15% [*Wang et al.*, 2001b]. Ozone for the chemiluminescent reaction with NO in the detector was generated from ultrahigh-purity oxygen in cylinder. The NO detector was calibrated using a standard addition technique [*Wang et al.*, 1996, 2001b] by adding a small amount (0.23 sccm) of the above mentioned standard to the ambient air stream (flow rate = 800 sccm, which gave a 4.3 ppbv of NO). The calibration was conducted every six hours in the spring and every eight hours in the summer phase. The mass flow controller/meter for the standard and sample were calibrated three times on site using a primary bubble flow calibration system (Sensidyne, Model Gilian Gilibrator), and the slope and the intercept from the multipoint calibrations showed a variation of less than 6% from April to July 2003. In addition, the small flow of the NO standard was directly measured with the flow calibration system, and the value agreed within 6% with the calculated value from the linear fit of the multipoint calibrations ($r^2 = 1.0000$). The sensitivity of the NO detector determined by the standard addition method was also compared to the results from those in multipoint calibrations by diluting the same NO standard with scrubbed ambient air with the use of a

dynamic calibrator (Environics Inc., Model 6100). The sensitivity from the two methods agreed within 10%.

[12] NO_y was detected using another chemiluminescence analyzer equipped with an externally placed molybdenum oxide (MoO) catalytic converter (TEI, Model 42C-Y Trace Level). NO_y was converted to NO on the surface of MoO at 350°C, and then measured by the chemiluminescent detector. The analyzer had a detection limit of 0.05 ppbv, with a 2-σ precision of 4% and an uncertainty of about 10% [*Wang et al.*, 2003]. The sensitivity of the NO_y analyzer (as NO) was determined on the basis of multipoint calibrations, which were conducted five times on site, through diluting the above mentioned standard with scrubbed ambient air using the dynamic calibrator. In addition, the sensitivity was checked on a daily basis by injecting a span gas containing 16 ppbv of NO. The sensitivity did not show obvious difference (less than 10%) from multipoint calibrations in both spring and summer phases. The conversion efficiencies of the MoO catalyst for NO_y species were checked daily by injecting 16 ppbv *n*-propyl nitrate (NPN), which indicated near complete conversion of NPN throughout the study period. The two mass flow controllers in the dynamic calibrator were calibrated three times on site using the bubble flow calibration system and showed constant results (difference <2%).

[13] Both NO and NO_y instruments had a capability of correcting instrument background (i.e., subtracting the signals from a prereaction chamber). To ensure the baseline was correctly determined, an ultra pure air (in cylinder purchased from Scott Marrin Inc., California) was introduced to the inlets of the two instruments (upstream of the MoO converter for NO_y). The results showed nondetectable baseline bias for NO (0.000–0.004 ppbv, n = 2) and a signal for NO_y (mean = 0.11 ppbv, s.d. = 0.14 ppbv, n = 9) which was very small relative to ambient NO_y mixing ratios at WLG. Therefore no further correction on the baseline was made.

[14] A data logger (Environmental Systems Corporation, Model 8816) was used to control the calibrations and to collect data, which were averaged over 1-min intervals. The data presented in this study are hourly averaged values.

2.3. Calculation and Cluster Analysis of Back Trajectories

[15] To learn about the origins and transport pathways of air masses sampled, three-dimensional backward trajectories were calculated with the output from the simulations of a mesoscale meteorological model. Previous studies have shown that this method (i.e., considering three-dimensional movements of air parcels using meteorological data from a dynamically consistent numerical model) gives much more accurate trajectories of air masses [*Fuelberg et al.*, 1996; *Stohl*, 1998]. Using the PSU/NCAR mesoscale model MM5, we conducted meteorological simulations every 5 days for the whole study period. The model was run in two nesting domains with a horizontal grid spacing of 81 km and 27 km, respectively, using the two-way nesting techniques. The two simulation domains covered nearly the whole Eurasian continent including China. The initial and boundary conditions were generated from NCEP/FNL data on 26 pressure levels with a horizontal resolution of 1 by 1 degree, enhanced by using surface meteorological observation and radiosonde data for Asia. To reduce the forecast error, one four-dimensional data assimilation (FDDA) method, "analyses nudging," was employed in the outmost domain during the simulation.

[16] With the output of mesoscale simulations, 10-day back trajectories, terminated at 500 m above the ground level (AGL) of the peak of WLG, were calculated every 2 hours using the Hybrid Single-Particle Lagrangian Integrated Trajectory, Version 4.7 (HYSPLIT4 model) developed by the National Oceanic and Atmospheric Administration (NOAA) Air Resources Laboratory (R. R. Draxler and G. D. Rolph, HYSPLIT (Hybrid Single-Particle Lagrangian Integrated Trajectory) Model, 2003, access via NOAA ARL READY Web site at http://www.arl.noaa.gov/ready/hysplit4.html). The trajectories were calculated using nesting meteorological data. To identify the major patterns of transport, we applied cluster analysis, a multivariate statistical technique, to split the trajectories set into a number of groups using the statistical software SPSS. The positions of endpoints (i.e., latitude, longitude, and pressure) at 3-hour intervals for the previous 10 days were chosen as the clustering variables. This accounted for the variations in transport speed and direction in both the horizontal and vertical directions simultaneously, yielding clusters of trajectories of similar length, altitude, and curvature [*Harris and Kahl*, 1990]. With a total of 240 variables ($3 \times 8 \times 10$), about 850 back trajectories were segregated into clusters using the hierarchical Ward's method with a squared Euclidean measure. This clustering technique has been successfully used by other researchers [e.g., *Moody et al.*, 1995].

3. Results and Discussion

3.1. Overall Results and a Comparison With Other Locations

3.1.1. Temporal Variations and Overall Statistics

[17] Time series of hourly mixing ratios of O_3, CO, NO, and NO_y are shown in Figures 2a and 2b, together with some meteorological parameters for 20 April to 23 May 2003 and 15 July to 16 August 2003, respectively. Inspections of Figure 2 revealed that two major types of air masses were sampled during the study periods. One is the air mass influenced by anthropogenic pollution, characterized by sharp rises in the levels of CO, a tracer of combustion sources, and sometimes by the abundance of NO_y, which is also emitted when fossil fuels are burned. Air masses of this type contained a relatively high amount of water vapor and variable but generally lower mixing ratios of ozone. Examples of these polluted air masses can be illustrated by data collected on 21–22 and 26–27 April, 6–8 and 19 May, 18 and 26–27 July, and 9 and 13 August. These events are marked with the symbol "P" in Figure 2. Back trajectories (to be discussed in section 3.2) and wind data (in Figure 2) indicated that they often came from the northeast and east, consistent with the fact that the urban areas of Xi'ning and Lanzhou are situated in those directions. Another type of air mass had characteristics of the upper troposphere, such as being high in O_3, and low in CO and water. Examples of these air masses are illustrated by the data for 23–25 and 28–30 April, 16–17, 20–24 and 28 July, and 15–17 August. They are marked with inverted triangles in Figure 2. Back

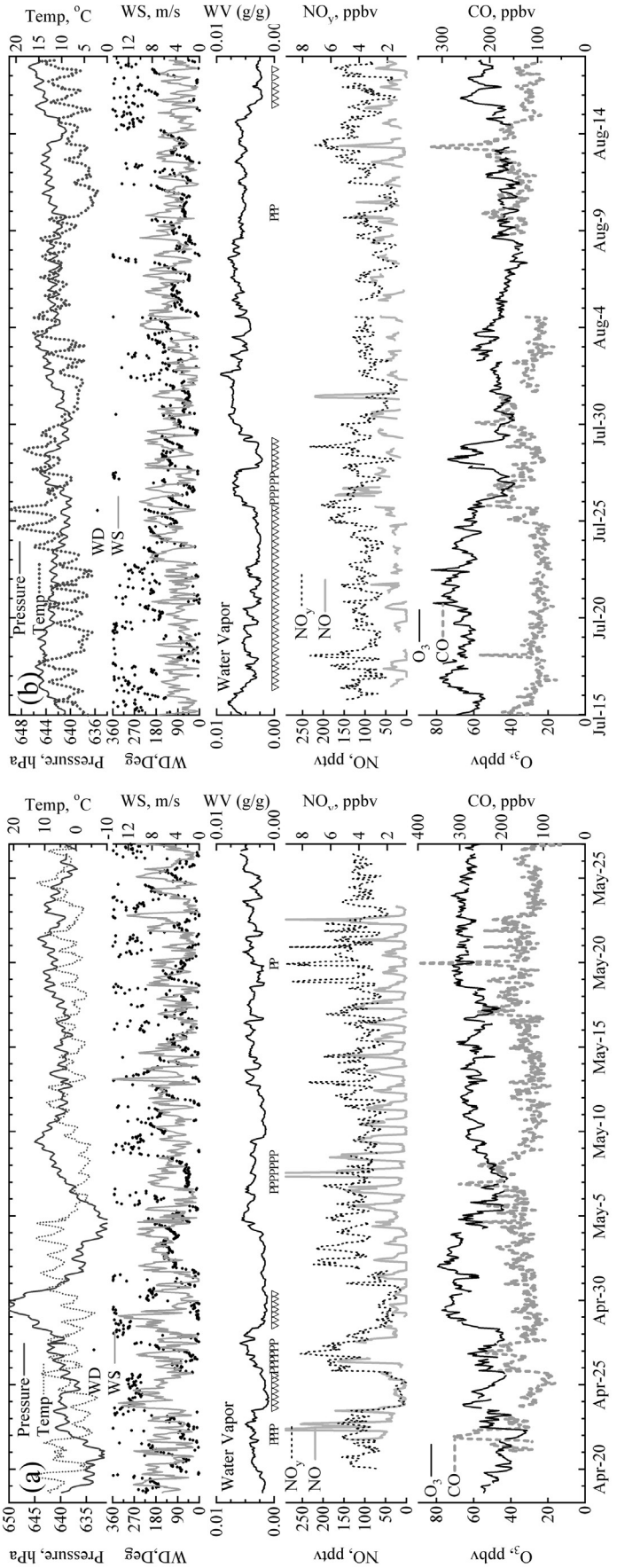

Figure 2. Time series of O_3, CO, NO, NO_y, and meteorological parameters measured at WLG in (a) spring and (b) summer. WS, wind speed; WD, wind direction; Temp, temperature; WV, water vapor; the periods of pollution plumes (indicated by P) and upper tropospheric air (inverted triangle icon) are marked.

Table 1. Summary of Hourly Data for Spring and Summer Phases[a]

	All Data		Upslope[b]		Downslope[b]	
	Mean	n	Mean	n	Mean	n
			Spring			
CO	155 (41)	757	147 (32)	373	164 (47)	384
NO_y	3.83 (1.46)	776	3.70 (1.29)	380	3.95 (1.60)	396
NO	43 (65)	707	72 (79)	355	13 (19)	352
O_3	58 (9)	749	58 (9)	367	59 (10)	382
			Summer			
CO	125 (36)	653	122 (35)	320	127 (36)	333
NO_y	3.60 (1.13)	744	3.82 (1.01)	372	3.39 (1.20)	372
NO	–	–	47 (32)[c]	339	–	–
O_3	54 (11)	723	53 (12)	363	54 (11)	360

[a]Mean (standard deviation) values are in ppbv, except for NO, which is in pptv; *n* is number of hourly data.

[b]Upslope equals 0800–1959 local time (Beijing Time); downslope equals 2000–0759 local time.

[c]Only upslope data in summer are shown for NO because of small sample size of the downslope data set.

trajectories and wind data show that these air masses predominantly arrived at the site from the west.

[18] Table 1 summarizes statistics on O_3, CO, NO, and NO_y, including mean, standard deviation, and number of data points (hourly values). The statistics are calculated for both study periods and for upslope (0800–1959 local time (LT) (Beijing Time)) and downslope (2000–0759 LT) according to the changes in vertical winds (see Figure 3). The average concentrations of CO, NO_y, and O_3 were higher in late spring than in summer. For example, the average CO level in spring was 155 ± 41 (standard deviation) ppbv compared to 125 ± 36 ppbv in the summer; O_3 was 58 ± 9 ppbv in spring compared to 54 ± 11 ppbv in summer. A z-test suggests that the differences in the levels of trace gas between the two periods of study were significant (at $p = 0.05$). The differences between the two periods will be further discussed with the aid of trajectory analysis. The discussion on diurnal difference will be given in section 3.1.3.

3.1.2. Comparison With Other Mountain Sites

[19] To place our observations in a global perspective, we compared the levels of trace gases at WLG with those from other remote, high-altitude sites. Table 2 summarizes the mean/median values of O_3, CO, and NO_y observed at WLG (this study), Mount Cimone (Italy, 2165 m), Mondy (Siberia, 2006 m), Jungfraujoch (Alps, Switzerland, 3580 m), Idaho Hill (Colorado, United States, 3070 m), Mauna Loa (Hawaii, United States, 3400m), Niwot Ridge (Colorado, United States, 3050 m), and the TRACE-P aircraft study.

[20] In general, the CO and O_3 levels at WLG were comparable to the levels measured at other continental mountain sites. For example, during the spring period, the average mixing ratio of CO was 155 ppbv, compared to 174 ppbv at Mount Mondy and Mount Jungfraujoch; the level of O_3 at WLG was 58 ppbv compared to 53 ppbv and 58 ppbv at Mondy and Jungfraujoch, respectively. (However, lower levels of CO and O_3 were observed at Mondy during the summertime.) Compared to the observations over the Pacific Ocean, similar concentrations of CO and O_3 were observed at WLG as onboard the

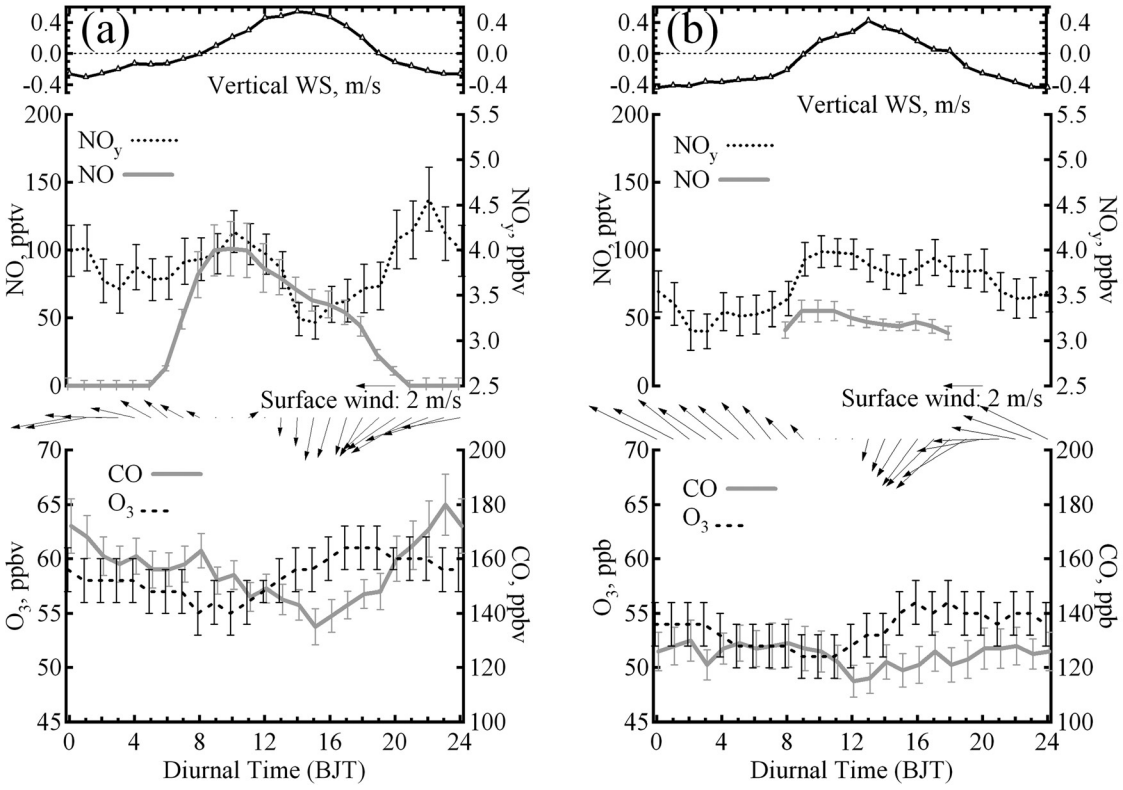

Figure 3. Average diurnal patterns of O_3, CO, NO, NO_y, and surface winds at WLG for (a) spring and (b) summer; error bars indicate standard errors.

Table 2. Comparison With Other Mountain Sites[a]

	Period	CO	O_3	NO_y	Altitude, m asl	Latitude, Longitude	Reference[b]
Waliguan	Apr-May 2003, Jul-Aug 2003	155 125	58 54	3.83 3.60	3816	36.28°N, 100.9°E	1
Mount Cimone	Jun 2000	121	58	1.15	2165	44.18°N, 10.7°E	2
Mondy	Mar-May 1999, Jun-Aug 1999	174 95	53.4 42.0		2006	51.65°N, 100.92°E	3
Jungfraujoch	Mar-May 1997-1999, Jun-Aug 1997-1998	174 129	58 58	1.10 0.81	3580	46.55°N, 7.98°W	4
Idaho Hill	Sept-Oct 1993	97	51	1.76	3070	39.5°N, 105.37°W	5
Mauna Loa (free tropospheric air)	Apr-May 1992, Jul-Aug 1992	129 68.5	63 38.9	0.37 0.20	3400	19.54°N, 155.58°W	6
Niwot Ridge (median)	Jul-Aug 1989	121	51		3050	40.03°N, 105.53°W	7
Niwot Ridge (mean/median)	Jun-July 1984			2.0/1.1	3050	40.03°N, 105.53°W	8
TRACE-P (Coastal 2–4km)	Feb-Apr 2001	151	58	0.43	2000–4000	20°–40°N, 90°–130°E	9

[a]All data are mean values in ppbv unless otherwise specified.
[b]References: 1, this study; 2, *Fischer et al.* [2003]; 3, *Pochanart et al.* [2003]; 4, *Zellweger et al.* [2003]; 5, *Williams et al.* [1997]; 6, *Atlas and Ridley* [1996]; 7, *Chin et al.* [1994]; 8, *Fahey et al.* [1986]; 9, *Russo et al.* [2003].

TRACE-P aircraft in spring 2001 (CO = 151 ppbv, O_3 = 58 ppbv) in the "coastal" air mass group (20°–40°N, 2–4 km asl). A lower level of CO (129 ppbv) was observed in Mauna Loa and a slightly higher level of O_3 (63 ppbv) in spring, but much lower levels of both CO (69 ppbv) and O_3 (39 ppbv) in summer. The latter reflects the fact that Mauna Loa is less impacted by sources of pollution in the Asian continent during the summer.

[21] Although the levels of CO and O_3 at WLG were generally comparable to those at other continental mountain sites, the NO_y concentrations at WLG (3.83 ppbv in spring and 3.60 ppbv in summer) were substantially higher. For example, 1.15 ppbv (in summer) were observed at Mount Cimone, 0.81 ppbv (in summer) and 1.10 ppbv (in spring) at Mount Jungfraujoch, and 2.0 ppbv (in summer) at Niwot Ridge. Much lower NO_y concentrations were measured at Mauna Loa (0.20–0.37 ppbv) and on TRACE-P aircraft (0.43 ppbv). The reasons for the unusually high NO_y at WLG will be discussed in section 3.3.

3.1.3. Diurnal Patterns

[22] Diurnal variations in the concentration of trace gases at mountaintop sites have been found to be closely related to mountain valley breezes [e.g., *Greenberg et al.*, 1992; *Oltmans and Levy*, 1994; *Fischer et al.*, 1998]. During daytime, solar radiation heats the air adjacent to the mountain slopes, resulting in an upslope flow that can bring air from the boundary layer. Shortly after sunset, radiative cooling of the slopes cools the adjacent air, causing a reversal of the flow (downslope), which can transport air masses from the free troposphere.

[23] In remote mountaintop sites such as Mauna Loa and Izaña, the concentrations of trace gases emitted by sources in the boundary layer, such as CO and hydrocarbons, often increase during daytime as O_3 values decrease and moisture increases; at night, lower trace gas and moisture levels are observed with increasing amounts of O_3 due to the downward transport of the free troposphere air [*Greenberg et al.*, 1992; *Oltmans and Levy*, 1994; *Fischer et al.*, 1998]. In polluted regions, however, a different diurnal pattern could emerge. For example, at Niwot Ridge, higher levels of O_3 and O_3 precursors were found in the afternoon because of the upslope transport of urban Denver plumes to the site [e.g., *Fahey et al.*, 1986; *Parrish et al.*, 1986, 1990].

[24] Figures 3a and 3b show average diurnal mixing ratios (and standard errors) of ozone, CO, NO, NO_y, and surface winds (both horizontal and vertical) at WLG for the present study. Similar to other mountaintop sites, upslope flow (represented by positive speeds) and downslope winds are clearly shown in both spring and summer. For trace gases, the mixing ratios of CO and NO_y in spring showed a minimum (CO = ~140 ppbv; NO_y = ~3.2 ppbv) in the afternoon (1400–1600 LT) and increased at night (CO = 160–180 ppbv; NO_y = 3.5–4.5 ppbv); NO_y showed an apparent morning peak coinciding an O_3 minimum, implying a local source of NO_y. In summer, CO had a similar profile to that in spring, while NO_y showed a broad daytime maximum. The day-night differences for both NO_y and CO were smaller in summer than in spring. As CO is mainly emitted from anthropogenic sources such as the burning of fossil fuels and biomass, the higher nighttime levels imply the transport of pollution. This attribution is supported by strengthening N-NE winds at night in springtime, which could transport pollutants to the site from the urban areas of Xi'ning and Lanzhou and from other pollution sources in that wind sector. Another possible cause for the elevated nighttime concentrations of CO (and NO_y) in spring was the transport of biomass-burning emissions in central Asia associated with large-scale descending motions. This topic will be discussed in more detail later in section 3.2.2.2. For the summer season, the elevated daytime level of NO_y, which contrasts with the CO pattern, suggests a different source of reactive nitrogen from that of CO.

[25] As for ozone, it had a similar diurnal pattern in the two phases, exhibiting low levels in the morning and enhanced levels in the late afternoon and at nighttime, with a diurnal difference of 4–5 ppbv. The lower morning values may be due to the depositional loss of ozone in stagnant air during the nighttime and early morning hours, and its enhancement in the afternoon could be due to the in situ photochemical production of ozone. *Tang et al.* [2002] also found a minimum in the concentrations of hydrogen peroxide during morning at this site.

[26] The NO levels showed a daytime maximum (~70 pptv in spring and ~50 pptv in summer) due to the photolysis of NO_2 to NO and perhaps to a stronger emission of NO from soils at daytime. (For most nights of the summer study, the NO detector was switched to the low-sensitivity mode, i.e., using

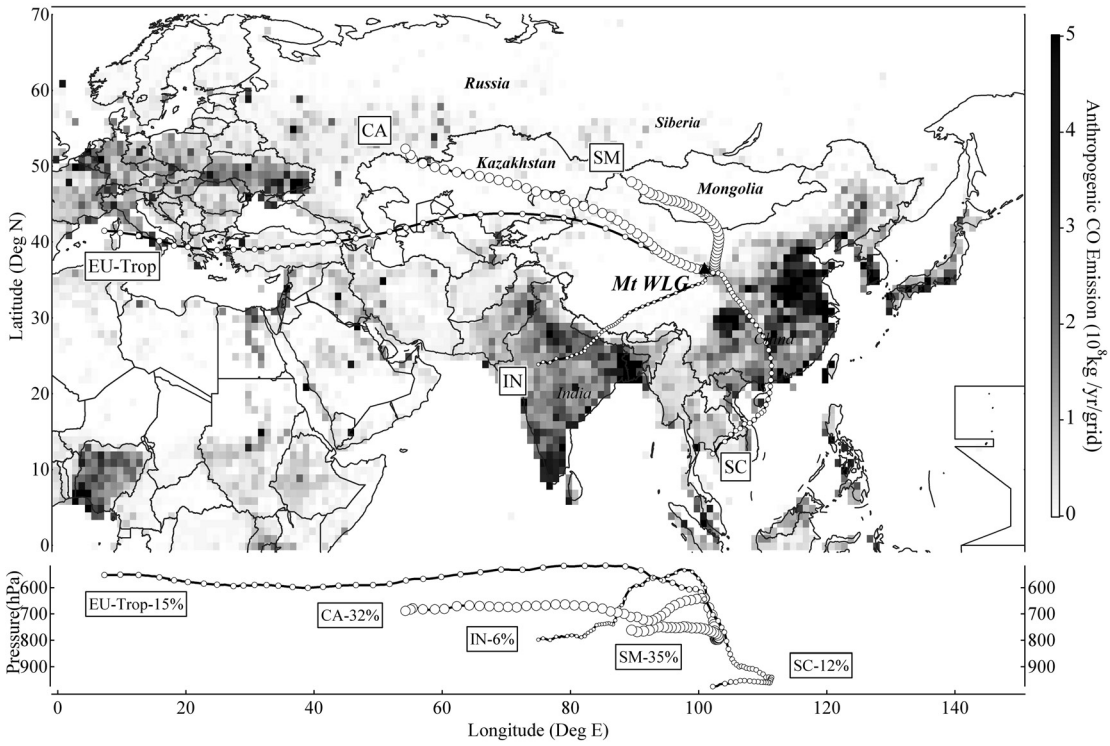

Figure 4. Ten-day mean trajectory clusters plotted on anthropogenic CO emissions (taken from the Emission Database for Global Atmospheric Research (EDGAR) Version 2.0 for year 1995). The open circles on the trajectories indicate 6-hour intervals. The size of the markers indicates the percentage of the particular cluster. Air mass groups: EU-Trop, eastern Europe/middle troposphere; CA, central Asia; SM, Siberia/Mongolia; IN, Indian subcontinent; SC, southern China.

indoor air as the source to generate ozone, in order to conserve the limited supply of pure oxygen.) These daytime concentrations imply that the NO levels at WLG are high enough to sustain a net photochemical formation of ozone [*Duderstadt et al.*, 1998; *Carpenter et al.*, 2000; *Ma et al.*, 2002; *Mihelcic et al.*, 2003] in both spring and summer. This result inferred from the in situ NO measurement is in contrast to the conclusion of a previous modeling study by *Ma et al.* [2002] that suggested a net photochemical destruction of O_3 at WLG in July. That study used NO_2 data obtained in 1996 using the filter packs/ion chromatography method to constrain a time-dependent box model. The filter data showed a NO_2 mixing ratio of 48 pptv in July with a model-calculated noontime NO value of 13 pptv and 19 pptv for free tropospheric air and boundary air mass, respectively. Our measurement in July-August 2003, however, suggests twice as much NO as in the model. It is not clear whether the difference in these two studies was due to an increase in NO_x emissions from 1996 to 2003 or to a possible problem with measurements using the filter-based method. The inferred positive contribution from photochemistry in our study is also in disagreement with the conclusion of a chemical transport model study by *Zhu et al.* [2004], which also suggested that there is a net destruction of ozone at WLG in summer. The discrepancy in these studies points to the importance of in situ measurements of NO using a high-sensitivity instrument for determining the role of photochemistry in the ozone budget.

3.2. Relation to Air Mass Transport

3.2.1. Patterns of Long-Range Transport

[27] Using the clustering technique described in section 2.3, all back trajectories for the two intensive periods were classified into five categories. Figure 4 gives the 10-day mean trajectories of the five clusters plotted on anthropogenic CO emissions taken from the Emission Database for Global Atmospheric Research (EDGAR) Version 2.0 for year 1995. Open circles on the trajectories indicated 6-hour intervals, with the size of the marker showing the percentage of the particular cluster. These five trajectory groups are described as follows: EU-Trop, air masses coming from the west that originated from eastern Europe and traveled at fast speeds in the middle troposphere over central Asia before subsiding to the site; CA, air masses coming from the northwest that originated from central Asia and transported in the lower troposphere passing over Kazakhstan and Xinjiang region of China; SM, air masses coming from the north that originated from western Siberia and Mongolia and moved in a southerly/southeasterly direction over Inner Mongolia and Gansu province of China at lower speeds; IN, air masses originating from India that climbed over the Qinghai-Tibetan Plateau; and SC, air masses originating from south Asia that passed through the planetary boundary layer over southern and central China. It can be seen from anthropogenic CO emissions that the trajectories coming from the west passed over a large remote area with very few anthropogenic emissions.

Table 3. Classification Results of Trace Gases in Different Trajectory Groups[a]

	Whole Period				Spring				Summer			
	CO	NO_y	O_3	WV[b]	CO	NO_y	O_3	WV[b]	CO	NO_y	O_3	WV[b]
EU-Trop	121 (38)	3.25 (1.28)	60 (9)	2.9 (1.5)	133 (27)	2.88 (1.39)	61 (11)	2.6 (0.8)	103 (20)	3.74 (0.91)	58 (9)	4.1 (1.4)
CA	129 (37)	3.75 (1.33)	60 (10)	3.4 (1.3)	146 (38)	3.76 (1.57)	59 (9)	2.8 (1.2)	113 (27)	3.74 (1.08)	60 (10)	3.9 (1.2)
SM	157 (45)	3.96 (1.29)	54 (10)	4.2 (1.2)	161 (44)	4.09 (1.23)	56 (9)	3.8 (1.0)	144 (45)	3.60 (1.36)	49 (10)	5.4 (1.1)
IN	146 (32)	4.24 (1.20)	57 (11)	4.2 (1.7)	157 (27)	4.45 (1.23)	61 (9)	3.3 (1.4)	121 (30)	3.83 (1.08)	46 (8)	5.9 (1.0)
SC	150 (29)	3.36 (1.21)	45 (9)	6.3 (1.4)	154 (36)	4.41 (1.48)	68 (9)	3.8 (2.3)	149 (29)	3.30 (1.17)	44 (6)	6.5 (1.1)

[a]Values are mean (standard deviation) in ppbv unless otherwise specified.
[b]WV, water vapor (units are $\times 10^{-3}$ g/g).

[28] Among the five trajectory groups, SM and CA occurred the most, accounting for 35% and 32% of the total, respectively, followed by EU-Trop (15%), SC (12%), and IN (6%). For the spring period, SM accounted for 46%, while the most dominant group in summer was CA (37%) (see also Figure 6). The SC air mass occurred mainly in summer, accounting for 25% compared to 2% in spring, reflecting the increased impact of Asian monsoons on the Asian interior region. The percentage of distribution of the trajectory clusters is generally consistent with the results of the wind rose analysis for these seasons at this site [e.g., *Zhou et al.*, 2003], but the trajectories are expected to provide more information on the histories (i.e., origin and transport path) of the air masses arriving at WLG.

3.2.2. Chemical Characteristics of Air Masses

3.2.2.1. Overall Statistics on the Characteristics of Air Masses

[29] To gain insights into the chemical characteristics of each of the above five categories of air mass, hourly data on concentrations of trace gas (and water vapor) were sorted according to the trajectory clusters. The statistics are given in Table 3 for whole study period and for the spring and summer phases separately. It can be seen that the mean water vapor content in different trajectory clusters is consistent with the vertical movement of these clusters: subsiding EU-Trop contained the least amount of water vapor (2.6×10^{-3} g/g in spring and 4.1×10^{-3} g/g in summer), indicating the success of trajectory calculations and cluster analysis in characterizing the vertical movements of air parcels. CA, which passed over vast regions of deserts of Xinjiang, also had less water vapor ($\sim 3.4 \times 10^{-3}$ g/g) than air masses originating in the south or northeast (i.e., SM, IN and SC).

[30] Overall, the air masses from the remote western regions (EU-Trop and CA) contained the lowest levels of CO (mean = 121–129 ppbv), but had the highest O_3 mixing ratio (60 ppbv), compared to the other three air mass groups SM, IN, and SC (mean O_3 = 45–57 ppbv; CO = 146–157 ppbv). The NO_y levels in EU-Trop and CA were also somewhat lower, but the differences were not as significant as in the case of CO. The higher concentrations of CO in types SM, IN, and SC indicate some contributions of anthropogenic emissions from eastern and southern China, and possibly from India.

[31] Considering seasonal variations, a higher average level of CO was found in the spring period for each air mass group. For example, the mean (plus or minus standard deviation) CO mixing ratio in the CA air mass was 146 (±38) ppbv in spring compared to 113 (±27) ppbv in summer. The higher springtime CO may be due to a longer lifetime of CO against hydroxyl radicals in spring compared to summer. The average O_3 levels were also higher in spring, except for air mass CA, which had a comparable mean O_3 value in spring and summer (59 ± 9 versus 60 ± 10 ppbv). In fact, the highest average O_3 in summer among the five air mass groups was found in the CA group. A scatterplot of O_3 versus CO (Figure 5) shows that O_3 was negatively correlated with CO, suggesting that the high ozone in summer in the CA group was mostly due to the transport of upper tropospheric/lower stratospheric air, not of anthropogenic pollution. (The overall weak negative O_3-CO correlations were also indicated in other air mass groups; figures not shown.) Examination of three-dimensional potential vorticity based on MM5 simulations provided dynamic evidence of the stratospheric origin for most summertime high-ozone cases, which were related to upper level trough along subtropical jet stream [*Ding and Wang*, 2006]. For NO_y, a higher level was found in the spring phase, possibly due to air masses of regional pollution (i.e., SM, IN, and SC), but the air masses that originated from the west (EU-Trop and CA) had higher or comparable average NO_y concentrations in summer in spite of the lowest CO contents, suggesting the presence of noncombustion sources of reactive nitrogen.

3.2.2.2. Air Masses Originating From the West: Signals of the Burning of Biomass in Central Asia in Spring 2003

[32] As shown in Table 3, the two groups of air masses arriving from the west (EU-Trop and CA) had the lowest average CO values, which can be considered the background levels for the middle and lower troposphere, respec-

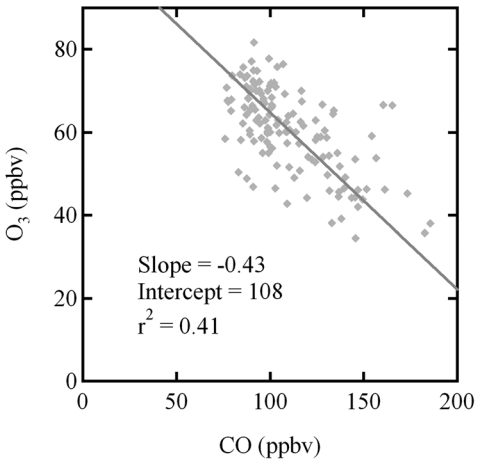

Figure 5. Scatterplot of O_3 versus CO for the CA air mass group in the summer period. The regression statistic is determined using the reduced major axis method.

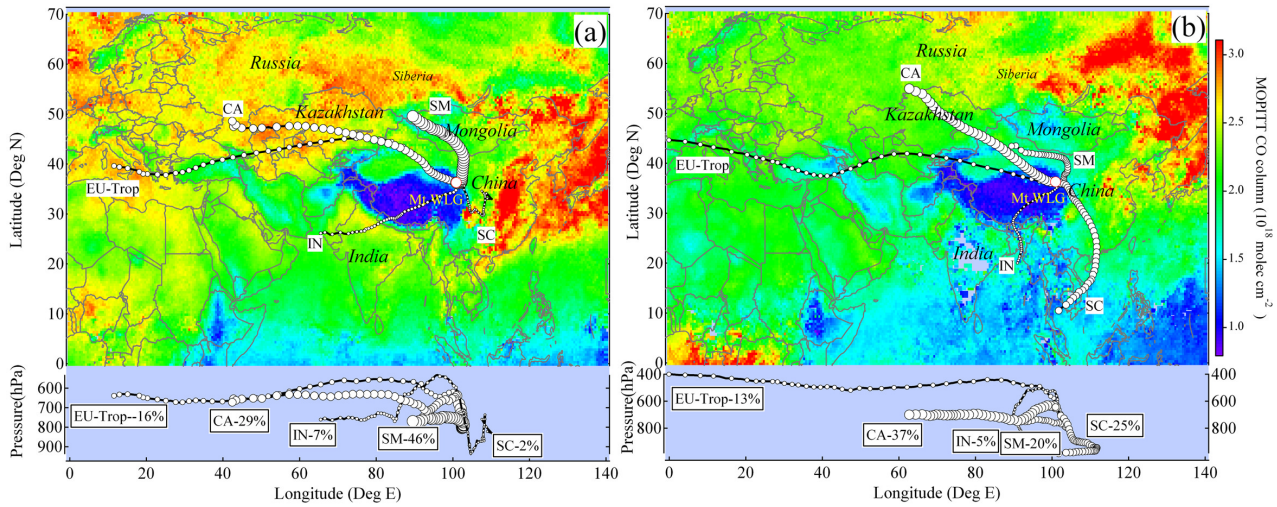

Figure 6. Mean CO column from MOPITT and trajectory clusters for (a) spring and (b) summer.

tively, in the interior Asian continent. These background concentrations are a combined result of the contributions from transcontinental transport from Europe and the emissions in the remote regions of central Asia and western China. Several recent studies have shown that wild forest fires in Siberia in spring and summer could significantly affect the background levels of trace gases on a regional or even global scale [*Kato et al.*, 2002; *Pochanart et al.*, 2003; *Honrath et al.*, 2004; *Jaffe et al.*, 2004]. Thus it is of great interest to investigate whether these burning activities had an impact on the levels of trace gases measured at WLG.

[33] To obtain information on fires and their possible impact on the regional distribution of CO, we examined fire detection data acquired by Moderate-Resolution Imaging Spectroradiometer (MODIS), via the Web site of Web Fire Mapper (http://maps.geog.umd.edu/). We also looked at the CO column data obtained from the Measurements of Pollution in the Troposphere (MOPITT) satellite for the same periods when we conducted measurements at WLG. Figures 6a and 6b show the mean CO column for the spring and summer periods, respectively. (The MODIS fire detection data are not shown here.) These remote-sensing data revealed very active biomass burning and the presence of high concentrations of CO in the border regions between Kazakhstan and Russia during the spring period, while during the summer study the burning of biomass was concentrated in eastern Siberia. To link the transport pathways with these biomass-burning regions, Figure 6 also shows the trajectory groups and their percentage of occurrence in the two study periods. It shows that the EU-Trop, CA, and SM air masses could be affected by the burning of biomass in the spring period, as WLG was downwind from those burning regions. In contrast, during the summer study, the forest fires mainly occurred in eastern Siberia, whose air masses were rarely transported to WLG (see Figure 6b). A comparison of the annual CO emission inventory (Figure 4) and the CO column data from MOPITT suggests that accurate data on the wild fires at the time of a field study are needed in order to explain the variations in measurement in downwind regions, which the annual average inventory cannot provide such information.

[34] Examinations of in situ measurements at WLG also revealed some impacts from the burning of biomass on the levels of trace gases in the air masses coming from the west during the spring period. The in situ measured CO showed some correlations with NO_y in EU-Trop and CA air masses (r^2 = 0.23–0.33), whereas their relationships were much weaker in summer (r^2 = 0.04–0.07, see Figures 7a–7d). Since CO is a tracer of combustion sources, the correlation in spring suggests that both species were contributed by combustion processes. Because the regions over which the EU-Trop and CA air masses passed were sparsely populated, the most likely contribution is the burning of biomass. The lack of correlation between CO and NO_y in summer is consistent with the minimum burning occurrence in central Asia (see Figure 6b). For the EU-Trop group, the low mean values of CO and NO_y but the best correlation between them suggests that these air masses coming from the west and subsiding from relatively high altitudes were occasionally influenced by biomass-burning plumes. Previous studies have found that plumes of biomass burning can penetrate the boundary layer into the middle troposphere or even to a higher level [*Folkins et al.*, 1997; *Kondo et al.*, 2004]. An examination of MOPITT CO data for different levels of pressure indeed indicated the presence of elevated concentrations of CO in the middle troposphere, especially over Kazakhstan (not shown).

[35] In search of more evidence of the impact from the burning of biomass, we examined data on nonmethane hydrocarbons (NMHCs) and halocarbons collected during this experiment. The CO in the air masses coming from the west (EU-Trop and CA) in the spring study showed a moderate correlation (r^2 = 0.34 and 0.37, respectively) with CH_3Cl, a known tracer of biomass burning [*Blake et al.*, 1996]. Moreover, we compared the ratios of ethyne to propane and benzene to propane in high-CO (>150 ppbv) and low-CO (<120 ppbv) cases in the EU-Trop air mass group. These species have a similar chemical lifetime (~12–18 days) against hydroxyl radicals, and are inefficiently removed by wet removal processes. Therefore the ethyne to propane and benzene to propane ratios should retain the characteristic of recent emission sources that had

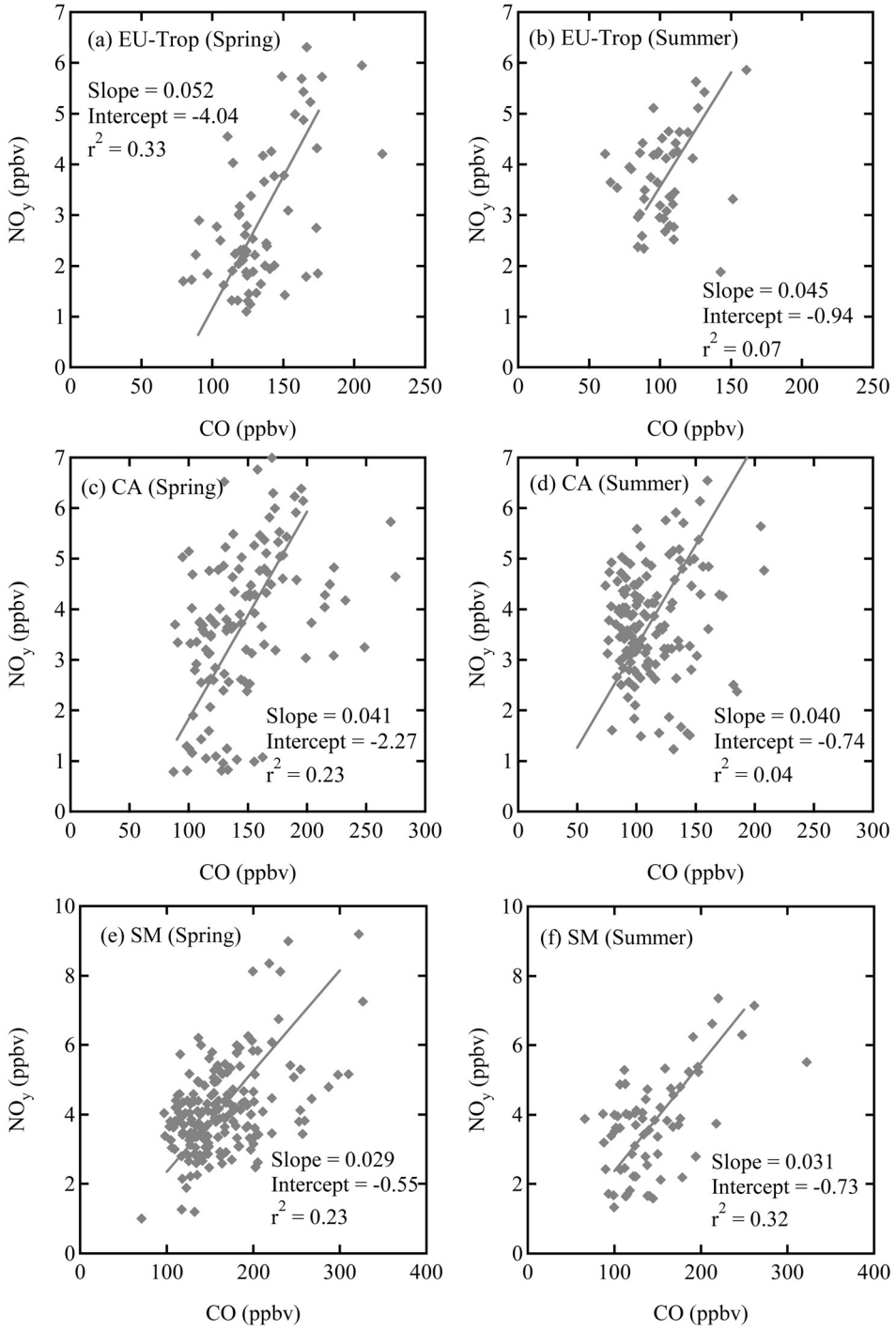

Figure 7. Scatterplots of CO versus NO_y: (a) spring EU-Trop, (b) summer EU-Trop, (c) spring CA, (d) summer CA, (e) spring SM, and (f) summer SM. The regression statistics are determined using the reduced major axis method.

been injected into the air masses. It is known that the burning of biomass produces more ethyne and benzene relative to propane compared to the burning of fossil fuels [*Carmichael et al.*, 2003a]. Thus these ratios can be used to check whether the high-CO cases in the descending EU-Trop air mass had a strong signal of biomass burning compared to the low-CO cases, which would be representative of unperturbed free troposphere air. It was found that the high-CO events in the EU-Trop did indeed have a higher mean ratio of ethyne/propane (1.65 ± 0.10 versus 0.96 ± 0.14). For benzene/propane, a slightly higher mean ratio was also indicated in the high-CO cases (0.34 ± 0.03 versus 0.25 ± 0.15). Such additional evidence suggests the contribution from the burning of biomass in the air mass coming from the west during the spring study. It is, however, difficult to quantify, using the measurements alone, the

impacts of the burning of biomass. Chemical transport model studies will be needed, but such studies are beyond the scope of the present work.

3.3. Sources of the High Concentrations of Reactive Nitrogen at WLG

[36] As mentioned in the above sections, during the study, the levels of NO_y at WLG were found to be particularly high when compared to those of other remote sites. In this section we discuss the possible reasons for the high concentrations of NO_y by considering the issues of measurements and emissions.

[37] As described in the experimental section, both NO and NO_y instruments were well calibrated during the study, and there were no indication of significant bias in baselines. However, it has been known that measurements of NO_y using catalytic converters can be subject to positive interferences due to the conversion of non-NO_y nitrogen compounds such as ammonia (NH_3). *Williams et al.* [1998] found that NH_3 was converted at an efficiency of 0 to 8% in three NO_y instruments using Mo converters (similar to the one used in the present study) when the converters were spiked with 35–114 ppbv of NH_3. *Fitz et al.* [2003] reported an average conversion efficiency of 11% for NH_3 (range: 1.5–26%), based on testing 11 Mo converters by sampling 56 ppbv of NH_3. The conversion efficiency was found to be independent of converter temperature. The manufacturer of the NO_y instrument states that the NH_3 conversion efficiency rises as the converter ages, according to *Fitz et al.* [2003]. The converter used in our study was newly installed at the beginning of measurement campaign.

[38] Ammonia was not measured during the present study, but according to a previous study carried out at WLG using passive samplers [*Carmichael et al.*, 2003b], the NH_3 mixing ratio was indeed quite high with a median value of 4 ppbv based on 6 monthly averaged samples. Such a value is comparable to that measured at a polluted rural site in central eastern China, Lin'an (mean = 5 ppbv) (see Figure 4 of *Carmichael et al.* [2003b]). Assuming a 10% NH_3 conversion efficiency in our instrument and a summertime ambient NH_3 of 8 ppbv (inferred from the observation at Lin'an showing summertime NH_3 twice of the annual average (see Figure 9 of *Carmichael et al.* [2003b])), the positive interference due to NH_3 would be as large as 0.8 ppbv. This is significant, but the high levels of NO_y of 3.4–4 ppbv measured at WLG still cannot be explained. Hence there must be some source(s) of reactive nitrogen in the study area that are not present near to other remote mountain sites. The presence of a source or sources of reactive nitrogen was also indicated by relatively high concentrations of NO, which were measured using an instrument not subject to the interference of ammonia. The daytime NO mixing ratio in the spring at WLG (mean = 72 pptv) is much higher than the TRACE-P aircraft measurement obtained at 2–7 km for the "central" source region (mean = 14 pptv) and at 2–4 km from the "coastal" source region (23 pptv) [*Russo et al.*, 2003].

[39] The major source of tropospheric reactive nitrogen (as NO_x) is fossil fuel combustion, followed by the burning of biomass, soil emissions, discharges of lightning, and the oxidation of ammonia [*Warneck*, 2000]. An inventory of emissions recently compiled by *Streets et al.* [2003] shows that power generation accounts for 39% of total NO_x emissions in China, followed by industry and transportation, both accounting for 25%, with other sources contributing 11%. Emissions from soils and discharges of lightning were not included in the estimate.

[40] A positive correlation between CO and NO_y is expected if combustion is the major source of these gases. Figure 7 indicates that there were some correlations (r^2 = 0.23–0.33) for the three dominant air masses in spring, while in summer no correlation was found between CO and NO_y ($r^2 < 0.1$) in the air masses of EU-Trop and CA, except for air mass SM, which may be attributed to the influence of regional pollution in the northeast. We also examined the scatterplots between NO_y and some NMHCs of anthropogenic origin, such as ethyne, benzene, and toluene, and obtained a similar result, namely, that there was little correlation between NO_y and these species in summer. These results point to the presence of noncombustion sources for NO_y, particularly in summer.

[41] What is (are) the likely noncombustion source(s) for the elevated NO_y at WLG? Lightning is unlikely to sustain a level of 4 ppbv of NO_y here because there are few storms in the drought-stricken regions of western China. The trajectory analysis given in the above section suggests that the burning of biomass had only a limited impact during the spring study. Here, we believe that emissions from soils related to animal waste is the most plausible noncombustion source contributing to the high NO_y (and NO) measured at WLG. It is known that nitrification and denitrification processes in soils can be a significant natural source of NO_x [*Williams et al.*, 1987; *Hargreaves et al.*, 1992; *Dunfield and Knowles*, 1999]. Nitrification converts N(-III) to N(V) through ammonium oxidizing nitrifiers, which convert NH_4^+ to NO_2^-, and through nitrite oxidizing nitrifiers, which oxidize NO_2^- to NO_3^-, whereas denitrification reduces NO_3^- to N_2 by which fixed N_2 is returned to the atmosphere. The amount of NO produced is closely related to the temperature, type, moisture, pH, and to the nitrate and ammonium contents of the soils [*Williams et al.*, 1988]. It has been found that fertilized soils and pastures give out particularly strong emissions of NO_x [*Kessel et al.*, 1992; *Williams et al.*, 1992; *Bolan et al.*, 2004].

[42] In Qinghai province (where WLG is situated), cattle grazing is a major activity, and many areas in the region are heavily fertilized with animal waste, which contain rich sources of urea and other N substances. (Cattle and sheep were indeed often observed around the study site during the summer months.) Hence it is quite possible that the high levels of NO_y observed at WLG were due to emissions of microbial activities in soils and, to a lesser extent, to the atmospheric oxidation of NH_3. This attribution is supported by the presence of unusually high concentrations of NH_3 at WLG whose sources would also emit NO [e.g., *Wang et al.*, 2004]. It is worth noting that the sharp drops in the concentrations of NO_y (to about 1.5 ppbv) on 31 July and 10 August were associated with decreases in temperature (see Figure 2), which may be an indicator of reduced emissions from soils at a lower temperature.

[43] We further estimated the amount of NO_x from soils related to animal waste and compared it to that from combustion sources in Qinghai province. We adopted the methods detailed by *Intergovernmental Panel on Climate*

Change [1996] for estimating N_2O and the rate of N excretion from different groups of animals. In year 2003, there were about 23 million livestock in Qinghai province [*Qinghai Bureau of Statistics*, 2004]. The N_2O emissions from soils were estimated to be 4.7 GgN in the Qinghai region. Assuming a NO to N_2O ratio of 3 [*Wang et al.*, 2004], the NO_x emissions related to animal waste would be 45.9 $GgNO_2$ in Qinghai in 2003, which is about 50% of the total amount of anthropogenic emissions of NO_x estimated by *Streets et al.* [2003]. This implies that the emission from soils is an important source of NO_x in Qinghai, and possibly for other less industrialized western provinces in China.

[44] An important question is what constituents may have contributed to the large abundances of NO_y at WLG. Many studies have shown that the major NO_y components in rural and remote areas are NO_x, peroxyacetyl nitrate (PAN), nitric acid, aerosol nitrate, and possibly also the collection of many alkyl nitrates. The daytime NO at WLG in summer is 47 pptv, and assuming a NO_2 to NO ratio of 7.1 [*Zellweger et al.*, 2000], NO_x would be about 0.38 ppbv. Previous measurements at WLG using filter packs indicated a mean mixing ratio of total nitrate (nitric acid + nitrate) of 0.8 ppbv in summer in 1997–1999 (and 1.1 ppbv in spring) with nitrate predominating [*Xue*, 2002]. These values are significantly higher than that obtained during springtime TRACE-P aircraft study (~0.42 ppbv) [*Russo et al.*, 2003; *Kondo et al.*, 2004] and from other remote continental sites in summer such as Niwot Ridge (0.08–0.31 ppbv) [*Fahey et al.*, 1986] and Jungfraujoch (0.23 ppbv) [*Zellweger et al.*, 2003]. In fact, the levels of NO and total nitrate (and NO_y) are more comparable to those observed in rural areas [e.g., *Parrish et al.*, 1993]. If we assume a typical rural value of 0.8 ppbv for PAN and the sum of alkyl nitrate of 0.5 ppbv [*Day et al.*, 2003], then the NO_x, total nitrate, PAN, and sum of alkyl nitrate could add up to 2.48 ppbv which would account for 70% of the summertime NO_y of 3.6 ppbv at WLG. The remaining could be contributed by the interference from NH_3 (and any unidentified interferences to the MoO converter) and by other minor NO_y species. The large total nitrate to NO ratio at WLG suggests a fast conversion of NO to NO_y by local photochemistry and/or long-range transport of NO_y via high altitudes with minimal loss of NO_y. Clearly, measurements of individual NO_y components as well as a more accurate determination of the interference due to NH_3 will be required to confirm the above estimates and to determine the partitioning of NO_y. Additional studies are also needed to pin down and better quantify source(s) of reactive nitrogen and to study the implications for atmospheric nitrogen cycles and the ozone chemistry of the background atmosphere in western China.

4. Summary and Conclusions

[45] Ozone, carbon monoxide, nitric oxide, and total reactive nitrogen, were continuously measured, along with the collection of canister/filter samples for hydrocarbons, halocarbons, and fine aerosols in late spring (20 April to 23 May) and summer (15 July to 16 August) in 2003 at WLG, a GAW baseline station located in the Qinghai-Tibetan Plateau. Here, we have reported continuously measured trace gases (O_3, CO, NO and NO_y) to examine their temporal behaviors, relationship to long-range transport, the influence of wild forest fires in central Asia, and the sources/origins of these gases.

[46] Ozone exhibited a diurnal cycle similar to that observed in remote mountain sites, i.e., a late morning minimum due to the depositional loss of O_3. CO and NO_y, on the other hand, showed enhanced concentrations at night, indicating the transport of combustion-related air masses to the study site. The CO levels at WLG were comparable to those at other remote mountain sites, but the NO_y concentrations were found to be substantially higher. The daytime NO mixing ratio (mean = 47–72 pptv) was high enough to sustain a net photochemical formation of O_3 at the remote site.

[47] Ten-day back trajectories show that the air masses sampled at WLG originated in Europe and traveled over vast, sparsely populated regions of central Asia/western China, from Mongolia and traveled through northern China, from southern China, or from the Indian subcontinent. While CO, a tracer of combustion sources, showed expected lower values in the air masses coming from the west, high concentrations of ozone were often associated with these air masses. This, together with the negative correlation of O_3 with CO, water vapor, and the NMHCs of anthropogenic origins in these air masses, implies that the high-ozone cases observed in this study were mainly due to the transport of upper troposphere air. In situ chemical measurements (CO-NO_y correlation, ethyne/propane, and benzene/propane), MOPITT and MODIS remote-sensing data revealed some impacts from strong forest fires in central Asia in late spring of 2003 on the background concentrations of trace gases over western China.

[48] An unexpected finding of this study is the much higher concentrations of NO_y (and to a lesser extent, NO) when compared to other remote environments. While more studies are needed to pin down these sources/causes, including a possible contribution from long-range transport, we believe that emissions from soils enhanced by animal waste were an important cause of the high NO_y. A preliminary estimate suggests that soil emissions could be comparable to combustion sources in the western provinces of China. Thus they may have important implications for the oxidative capacity and nitrogen chemistry of the atmosphere over the Qinghai-Tibetan Plateau.

[49] **Acknowledgments.** The authors would like to thank Steven Poon for his invaluable contribution to the preparation and execution of the field study. We thank Joey Kwok for his help in processing the in situ data, Shiguang Qin for processing the MOPITT satellite data, and Hai Guo for his comments. We are grateful to the staff at the WLG Observatory for their help throughout the field experiments and to NCAR and the NOAA Air Resources Laboratory (ARL) for providing the MM5 and HYSPLIT model, respectively. We thank Donald Blake for analyzing whole air samples collected in canisters and the NCAR MOPITT science team for providing remote-sensed CO data. This research was funded by the Research Grants Council of Hong Kong (project PolyU 5057/02E to Tao Wang) and by the Ministry of Science and Technology of China (project 2001DIA10009 to Jie Tang).

References

Atlas, E. L., and B. A. Ridley (1996), The Mauna Loa Observatory Photochemistry Experiment: Introduction, *J. Geophys. Res.*, *101*(D9), 14,531–14,542.

Blake, N. J., D. R. Blake, B. C. Sive, T. Y. Chen, F. S. Rowland, J. E. Collins Jr., G. W. Sachse, and B. E. Anderson (1996), Biomass burning emissions and vertical distribution of atmospheric methyl halides and other reduced carbon gases in the South Atlantic Region, *J. Geophys. Res.*, *101*(D19), 24,151–24,164.

Bolan, N. S., S. Saggar, J. F. Luo, R. Bhandral, and J. Singh (2004), Gaseous emissions of nitrogen from grazed pastures: Processes, measurements and modelling, environmental implications, and mitigation, *Adv. Agron.*, *84*, 37–120.

Carmichael, G. R., et al. (2003a), Evaluating regional emission estimates using the TRACE-P observations, *J. Geophys. Res.*, *108*(D21), 8810, doi:10.1029/2002JD003116.

Carmichael, G. R., et al. (2003b), Measurements of sulfur dioxide, ozone and ammonia concentrations in Asia, Africa, and South America using passive samplers, *Atmos. Environ.*, *37*, 1293–1308.

Carpenter, L. J., T. J. Green, G. P. Mills, S. Bauguitte, S. A. Penkett, P. Zanis, E. Schuepbach, N. Schmidbauer, P. S. Monks, and C. Zellweger (2000), Oxidised nitrogen and ozone production efficiencies in the springtime free troposphere over the Alps, *J. Geophys. Res.*, *105*(D11), 14,547–14,559.

Chin, M., D. J. Jacob, J. W. Munger, D. D. Parrish, and B. G. Doddridge (1994), Relationship of ozone and carbon monoxide over North America, *J. Geophys. Res.*, *99*(D7), 14,565–14,574.

Crutzen, P. J. (1973), A discussion of the chemistry of some minor constituents in the stratosphere and troposphere, *Pure Appl. Geophys.*, *106*, 1385–1399.

Danielsen, E. F. (1968), Stratosphere-troposphere exchange based on radioactivity, ozone and potential vorticity, *J. Atmos. Chem.*, *25*, 502–518.

Day, D. A., M. B. Dillon, P. J. Wooldridge, J. A. Thornton, R. S. Rosen, E. C. Wood, and R. C. Cohen (2003), On alkyl nitrates, O_3, and the "missing NO_y," *J. Geophys. Res.*, *108*(D16), 4501, doi:10.1029/2003JD003685.

Derwent, R., W. Collins, C. Johnson, and D. Stevenson (2002), Global ozone concentrations and regional air quality, *Environ. Sci. Technol.*, *36*(1), 379A–382A.

Ding, A., and T. Wang (2006), Influence of stratosphere-to-troposphere exchange on the seasonal cycle of surface ozone at Mount Waliguan in western China, *Geophys. Res. Lett.*, *33*, L03803, doi:10.1029/2005GL024760.

Duderstadt, K. A., et al. (1998), Photochemical production and loss rates of ozone at Sable Island, Nova Scotia during the North Atlantic Regional Experiment (NARE) 1 993 summer intensive, *J. Geophys. Res.*, *103*(D11), 13,531–13,555.

Dunfield, P. F., and R. Knowles (1999), Nitrogen monoxide production and consumption in an organic soil, *Biol. Fert. Soils*, *30*, 153–159.

Fahey, D. W., G. Hubler, D. D. Parrish, and E. Williams (1986), Reactive nitrogen species in the troposphere: Measurements of NO, NO_2, HNO_3, particulate nitrate, peroxacetyl nitrate (PAN), O_3 and total reactive odd nitrogen (NO_y) at Niwot Ridge, Colorado, *J. Geophys. Res.*, *91*(D9), 9781–9793.

Fischer, H., et al. (1998), Trace gas measurements during Oxidizing Capacity of the Tropospheric Atmosphere campaign 1993 at Izaña, *J. Geophys. Res.*, *103*(D11), 13,505–13,518.

Fischer, H., et al. (2003), Ozone production and trace gas correlations during the June 2000 MINATROC intensive measurement campaign at Mt. Cimone, *Atmos. Chem. Phys.*, *3*, 725–738.

Fitz, D. R., K. Bumiller, and A. Lashgari (2003), Measurement of NO_y during the SCOS97-NARSTO, *Atmos. Environ*, *37*(suppl. 2), S119–S134.

Folkins, I., R. Chatfield, D. Baumgardner, and M. Proffitt (1997), Biomass burning and deep convection in southeastern Asia: Results from ASHOE/MAESA, *J. Geophys. Res.*, *102*(D11), 13,291–13,299.

Fuelberg, H. E., R. O. Loring Jr., M. V. Watson, M. C. Sinha, K. E. Pickering, A. M. Thompson, G. W. Saches, D. R. Blake, and M. R. Schoeberl (1996), TRACE A trajectory intercomparison: 2. Isentropic and kinematic methods, *J. Geophys. Res.*, *101*(D19), 23,927–23,939.

Greenberg, J. P., P. R. Zimmerman, W. F. Pollock, R. A. Lueb, and L. E. Heidt (1992), Diurnal variability of atmospheric methane, nonmethane hydrocarbons, and carbon-monoxide at Mauna-Loa, *J. Geophys. Res.*, *97*(D10), 10,395–10,413.

Hargreaves, K. J., D. Fowler, R. L. Storeton-West, and J. H. Duyzer (1992), The exchange of nitric oxide, nitric dioxide and ozone between pasture and the atmosphere, *Environ. Pollut.*, *75*(1), 53–59.

Harris, J. M., and J. D. Kahl (1990), A descriptive atmospheric transport climatology for the Mauna Loa Observatory, using clustered trajectories, *J. Geophys. Res.*, *95*(D9), 13,651–13,667.

Honrath, R. E., R. C. Owen, M. Val Martin, J. S. Reid, K. Lapina, P. Fialho, M. P. Dziobak, J. Kleissl, and D. L. Westphal (2004), Regional and hemispheric impacts of anthropogenic and biomass burning emissions on summertime CO and O_3 in the North Atlantic lower free troposphere, *J. Geophys. Res.*, *109*, D24310, doi:10.1029/2004JD005147.

Intergovernmental Panel on Climate Change (1996), *Revised IPCC Guidelines for National Greenhouse Gas Inventories*, vol. 3, *Reference Manual*, chap. 4, pp. 4.1–4.125, Mexico City.

Jaffe, D., I. Bertschi, L. Jaegle, P. Novelli, J. S. Reid, H. Tanimoto, R. Vingarzan, and D. L. Westphal (2004), Long-range transport of Siberian biomass burning emissions and impact on surface ozone in western North America, *Geophys. Res. Lett.*, *31*, L16106, doi:10.1029/2004GL020093.

Kato, S., P. Pochanart, J. Hlrokawa, Y. Kajii, H. Akimoto, Y. Ozaki, K. Obi, T. Katsuno, D. G. Streets, and N. P. Minko (2002), The influence of Siberian forest fires on carbon monoxide concentration at Happo, Japan, *Atmos. Environ.*, *36*, 385–390.

Kessel, M., J. Grieser, W. Wobrock, W. Jaeschke, S. Fuzzi, M. C. Facchini, and G. Orsi (1992), Nitrogen oxides concentrations and soil emission fluxes in the Po Valley, *Tellus, Ser. B*, *44*, 522–532.

Kondo, Y., et al. (2004), Impacts of biomass burning in Southeast Asia on ozone and reactive nitrogen over the western Pacific in spring, *J. Geophys. Res.*, *109*, D15S12, doi:10.1029/2003JD004203.

Ma, J. Z., J. Tang, X. J. Zhou, and X. S. Zhang (2002), Estimates of the chemical budget for ozone at Waliguan Observatory, *J. Atmos. Chem.*, *41*(1), 21–48.

Mihelcic, D., et al. (2003), Peroxy radicals during BERLIOZ at Pabstthum: Measurements, radical budgets and ozone production, *J. Geophys. Res.*, *108*(D4), 8254, doi:10.1029/2001JD001014.

Monks, P. S. (2000), A review of the observations and origins of the spring ozone maximum, *Atmos. Environ.*, *34*, 3545–3561.

Moody, J. L., S. J. Oltmans, H. Levy II, and J. T. Merrill (1995), Transport climatology of tropospheric ozone: Bermuda, 1988–1991, *J. Geophys. Res.*, *100*(D4), 7179–7194.

National Research Council (1991), *Rethinking the Ozone Problem in Urban and Regional Air Pollution*, Natl. Acad. Press, Washington, D. C.

Oltmans, S. J., and H. Levy II (1994), Surface ozone measurements from a global network, *Atmos. Environ.*, *28*, 9–24.

Parrish, D. D., D. W. Fahey, E. J. Williams, and S. Liu (1986), Background ozone and anthropogenic ozone enhancement at Niwot Ridge, Colorado, *J. Atmos. Chem.*, *4*(1), 63–80.

Parrish, D. D., et al. (1990), Systematic variations in the concentration of NO_x (NO plus NO_2) at Niwot Ridge, Colorado, *J. Geophys. Res.*, *95*(D2), 1817–1836.

Parrish, D. D., et al. (1993), The total reactive oxidized nitrogen levels and their partitioning between the individual species at six rural sites in eastern North America, *J. Geophys. Res.*, *98*(D2), 2927–2939.

Pochanart, P., H. Akimoto, Y. Kajii, V. M. Potemkin, and T. V. Khodzher (2003), Regional background ozone and carbon monoxide variations in remote Siberia/east Asia, *J. Geophys. Res.*, *108*(D1), 4028, doi:10.1029/2001JD001412.

Qinghai Bureau of Statistics (2004), *Qinghai Statistical Yearbook 2004* (in Chinese), China Stat. Press, Beijing.

Russo, R. S., et al. (2003), Chemical composition of Asian continental outflow over the western Pacific: Results from Transport and Chemical Evolution over the Pacific (TRACE-P), *J. Geophys. Res.*, *108*(D20), 8804, doi:10.1029/2002JD003184.

Stohl, A. (1998), Computation, accuracy, and applications of trajectories: A review and bibliography, *Atmos. Environ.*, *32*, 947–966.

Streets, D. G., et al. (2003), An inventory of gaseous and primary aerosol emissions in Asia in the year 2000, *J. Geophys. Res.*, *108*(D21), 8809, doi:10.1029/2002JD003093.

Tang, J., Y. P. Wen, X. B. Xu, X. D. Zheng, S. Guo, and Y. C. Zhao (1995), China Global Atmosphere Watch Baseline Observatory and its measurement program, in *CAMS Annual Report 1994–95*, pp. 56–65, China Meteorol. Press, Beijing.

Tang, J., X. S. Zhang, X. D. Zheng, and J. Z. Ma (2002), The observational study of gaseous hydrogen peroxide at Mt. Waliguan (in Chinese), *Prog. Nat. Sci.*, *12*(2), 161–165.

Wang, T., et al. (1996), Ground-based measurements of NO_x and total reactive oxidized nitrogen (NO_y) at Sable Island, Nova Scotia, during the NARE 1993 summer intensive, *J. Geophys. Res.*, *101*(D22), 28,991–29,004.

Wang, T., T. F. Cheung, M. Anson, and Y. S. Li (2001a), Ozone and related gaseous pollutants in the boundary layer of eastern China: Overview of the recent measurements at a rural site, *Geophys. Res. Lett.*, *28*, 2373–2376.

Wang, T., Vincent T. F. Cheung, K. S. Lam, G. L. Kok, and J. M. Harris (2001b), The characteristics of ozone and related compounds in the boundary layer of the South China coast: Temporal and vertical variations during autumn season, *Atmos. Environ.*, *35*, 2735–2746.

Wang, T., A. J. Ding, D. R. Blake, W. Zahoroski, C. N. Poon, and Y. S. Li (2003), Chemical characterization of the boundary layer outflow of air pollution to Hong Kong during February-April 2001, *J. Geophys. Res.*, *108*(D20), 8787, doi:10.1029/2002JD003272.

Wang, Y. X., M. B. McElroy, T. Wang, and P. I. Palmer (2004), Asian Emissions of CO and NO_x: Constraints from aircraft and Chinese station data, *J. Geophys. Res.*, *109*, D24304, doi:10.1029/2004JD005250.

Warneck, P. (2000), *Chemistry of the Natural Atmosphere*, 2nd ed., Elsevier, New York.

Williams, E. J., D. D. Parrish, and F. C. Fehsenfeld (1987), Determination of nitrogen oxide emissions from soils: Results from a grassland site in Colorado, United States, *J. Geophys. Res.*, *92*(D2), 2173–2179.

Williams, E. J., D. D. Parrish, M. P. Butr, and F. C. Fehsenfeld (1988), Measurement of soil NO_x emissions in central Pennsylvania, *J. Geophys. Res.*, *93*(D8), 9539–9546.

Williams, E. J., G. L. Hutchinson, and F. C. Fehsenfeld (1992), NO_x and N_2O emissions from soil, *Global Biogeochem. Cycles*, *6*(4), 351–388.

Williams, E. J., J. M. Roberts, K. Baumann, S. B. Bertman, S. Buhr, R. B. Norton, and F. C. Fehsenfeld (1997), Variations in NO_y composition at Idaho Hill, Colorado, *J. Geophys. Res.*, *102*(D5), 6297–6314.

Williams, E. J., et al. (1998), Intercomparison of ground-based NO_y measurement techniques, *J. Geophys. Res.*, *103*(D17), 22,261–22,280.

Xue, H. S. (2002), Observational study of chemical characteristics of aerosol and trace gases of HNO_3, SO_2 at Mt. Waliguan (in Chinese), Master's thesis, Beijing Univ., Beijing, 19 Sept.

Zellweger, C., M. Ammann, B. Buchmann, P. Hofer, M. Lugauer, R. Ruttimann, N. Streit, E. Weingartner, and U. Baltensperger (2000), Summertime NO_y speciation at the Jungfraujoch, 3580 m above sea level, Switzerland, *J. Geophys. Res.*, *105*(D5), 6655–6667.

Zellweger, C., J. Forrer, P. Hofer, S. Nyeki, B. Schwarzenbach, E. Weingartner, M. Ammann, and U. Baltensperger (2003), Partitioning of reactive nitrogen (NO_y) and dependence on meteorological conditions in the lower free troposphere, *Atmos. Chem. Phys.*, *3*(3), 779–796.

Zhou, L. X., J. Tang, Y. P. Wen, J. L. Li, P. Yan, and X. C. Zhang (2003), The impact of local winds and long-range transport on the continuous carbon dioxide record at Mount Waliguan, China, *Tellus, Ser. B*, *55*, 145–158.

Zhu, B., H. Akimoto, Z. Wang, K. Sudo, J. Tang, and I. Uno (2004), Why does surface ozone peak in summertime at Waliguan?, *Geophys. Res. Lett.*, *31*, L17104, doi:10.1029/2004GL020609.

A. Ding, T. Wang, H. L. A. Wong, and W. S. Wu, Department of Civil and Structural Engineering, Hong Kong Polytechnic University, Hung Hom, Room TU702, Kowloon, Hong Kong, China. (cetwang@polyu.edu.hk)

J. Tang and X. C. Zhang, Key Laboratory for Atmospheric Chemistry, Centre for Atmosphere Watch and Services, Chinese Academy of Meteorological Sciences, 46 South Street, Zhongguan cun, Beijing 100081, China.